

A Multi-Hit mouse model to identify cooperating Ras effector pathways in lung cancer

Monica Musteanu^{1,2*}, Leander Blaas^{1*}, Rainer Zenz¹, Jasmin Svinka¹, Thomas Hoffmann¹, Beatrice Grabner¹, Daniel Schramek³, Hans-Peter Kantner¹, Mathias Müller⁴, Thomas Kolbe^{5,6}, Thomas Rüllicke⁵, Richard Moriggl¹, Lukas Kenner^{1,7}, Dagmar Stoiber^{1,8}, Josef Penninger³, Helmut Popper⁹, Emilio Casanova^{1*} and Robert Eferl^{1,10*#}

* equal contribution

¹ Ludwig Boltzmann Institute for Cancer Research, Waehringer Strasse 13a, A-1090 Vienna, Austria

² Spanish National Cancer Research Centre (CNIO), Melchor Fernández Almagro 3, E-28029 Madrid, Spain

³ Institute of Molecular Biotechnology, Dr. Bohr-Gasse 3, A-1030 Vienna, Austria

⁴ Institute of Animal Breeding and Genetics, University of Veterinary Medicine Vienna, Veterinaerplatz 1, A-1210 Vienna, Austria

⁵ Institute of Laboratory Animal Science and Biomodels Austria, University of Veterinary Medicine Vienna, Veterinaerplatz 1, A-1210 Vienna, Austria

⁶ Dept. Agrobiotechnology, IFA-Tulln, Biotechnology in Animal Production, University of Natural Resources and Applied Life Sciences, Konrad Lorenz Strasse 20, A-3430 Tulln, Austria

⁷ Clinical Institute of Pathology, Medical University of Vienna, Waehringer Guertel 18-20, A-1090 Vienna, Austria

⁸ Institute of Pharmacology, Center of Physiology and Pharmacology, Medical University of Vienna, Waehringer Strasse 13a, A-1090 Vienna, Austria

⁹ Institute of Pathology, Medical University of Graz, Auenbruggerplatz 35, A-8036, Graz, Austria

¹⁰ Institute for Cancer Research (ICR), Medical University of Vienna, Borschkegasse 8a, A-1090 Vienna, Austria

Conflicts of Interest: the authors disclose no conflicts.

Monica Musteanu: performed study, interpretation of data; Leander Blaas, Rainer Zenz, Jasmin Svinka, Thomas Hoffmann, Beatrice Grabner, Daniel Schramek: major technical support; Hans-Peter Kantner, Mathias Mueller, Thomas Kolbe, Thomas Rüllicke, Richard Moriggl, Lukas Kenner, Dagmar Stoiber, Josef Penninger: technical support; Helmut Popper: histopathological support and interpretation of data; Emilio Casanova: study concept and design, study supervision; Robert Eferl: study concept and design, interpretation of data, study supervision, wrote the manuscript.

to whom correspondence should be addressed:

Dr. Robert Eferl, Institute for Cancer Research & Ludwig Boltzmann Institute for Cancer Research, Waehringer Strasse 13a, A-1090 Vienna, Austria

Phone: +43 1 4277-64111

Fax: +43 1 4277-9641

E-Mail: robert.eferl@lbicr.lbg.ac.at

Abstract

We have established a mouse cancer model called Multi-Hit that allows evaluation of oncogene cooperativities in tumor development. The model harbours a Multi-Hit transgene for Cre-mediated stochastic introduction of several hits in a given tissue. Cells with cooperating hits are positively selected and give rise to tumors. We have used this approach to evaluate the requirement of Ras downstream effector pathways MAPK, RALGEF and PI3K in tumorigenesis. Ubiquitous, stochastic activation of Ras downstream effector pathways led to formation of typical Ras-induced tumors such as lung and pancreatic cancers. Tumor formation was accelerated upon deletion of the tumor suppressor protein PTEN. Application of a lung tissue-specific protocol revealed certain cooperativities of Ras downstream effector pathways in tumor initiation and invasiveness. Our results suggest that Multi-Hit mice can be used as an *in vivo* tool to identify oncogene cooperations in tumors that could be considered for combinatorial drug treatment therapies.

Introduction

Ras proteins are small GTP-hydrolyzing signaling proteins (GTPases) that exist in two functional conformations: active GTP-bound and inactive GDP-bound Ras. The intrinsic rates of GTP hydrolysis and nucleotide exchange by Ras proteins are slow and needs accessory proteins that enhance and regulate GDP-GTP cycling¹⁻⁵. Ras proteins are mutationally activated in many types of cancer including lung, pancreatic and colorectal cancer. The oncogenic Ras proteins harbour single amino acid missense mutations at residues G12, G13 or Q61 that render them constitutively active and often affect the cycling between the active GTP-bound and inactive GDP-bound state². Indirect mechanisms of Ras activation, such as loss of function of the NF1 tumor suppressor (a negative regulator of Ras) or by persistent activation of receptor tyrosine kinases are also seen in human cancers². In an activated state, Ras proteins exhibit high-affinity interactions with several downstream effector molecules that are implicated in cellular proliferation, differentiation and survival^{3, 6}. The best characterized Ras effector function is activation of Raf serine/threonine kinases (A-Raf, B-Raf and Raf-1) leading to stimulation of the MEK1/MEK2 and ERK1/ERK2 mitogen-activated protein kinase (MAPK) cascade. Initially, Raf was identified as a key downstream effector of Ras signalling⁷⁻¹⁰, and it was considered that the primary oncogenic function of Ras was mediated through Raf activation¹¹. However, the subsequent discovery of other Ras effector proteins suggested that oncogenic activities of Ras are mediated by both Raf-dependent and Raf-independent signalling. Among those signalling pathways, the RALGEF and PI3-Kinase (PI3K) pathways have attracted great attention and continuative studies have questioned the original dogma of Raf being the most important mediator of Ras in oncogenesis^{6, 12}. Currently, one of the most promising avenues in cancer therapy involves interfering with effector signalling networks downstream of Ras¹³. Therefore, it is an important issue to validate cooperativities of Ras downstream effectors as potential targets for cancer therapy.

Tumors arise from selected cells that have accumulated several mutations or hits in protooncogenes such as Ras or tumor suppressor genes such as PTEN leading to establishment of cellular characteristics known as “hallmarks of cancer”¹⁴⁻¹⁶. The underlying positive selection process leads to “survival of the fittest” tumor cells that have received potentially cooperating mutations. Here we report about a Multi-Hit mouse model that mimics positive selection of cooperating mutations and used this model to investigate Ras downstream effector pathways under competitive conditions in tumor formation.

Results

The Multi-Hit principle

We have developed a Multi-Hit mouse model that takes positive selection of cooperating oncogenes during tumor formation into account (Fig. 1a). The approach employs Cre-mediated inversion of expression units thereby randomly activating putative oncogene combinations in a given tissue. Cells with tumor-promoting activation patterns have a selective advantage to give rise to tumors. Moreover, combined approaches could employ additional hits (e.g. pretreatment of mice with carcinogenes) (Suppl. Fig. 1). For ease of use, we have established a recombineering method for rapid assembly of complex Multi-Hit BAC constructs (Fig. 1b)^{17, 18}.

Establishment of Ras effector (RasE) Multi-Hit mice

We established a Ras effector (RasE) Multi-Hit mouse model to dissect the requirement of Ras downstream effector pathways in tumorigenesis. The RasE Multi-Hit BAC contained expression units for S35, G37 and C40 H-rasV12 alleles insulated by chicken 2xHS4 sequences (Fig. 2a). These oncogenic H-ras mutant alleles carry individual mutations in the Ras effector domain and are surrogates for Ras-induced selective activation of MAPK (S35), RALGEF (G37) and PI3K (C40) downstream effector pathways^{12, 19, 20}. For simplicity, we indicate S35/MAPK, G37/RALGEF and C40/PI3K alleles with letters M, R and P, respectively. According to the Multi-Hit principle, Cre induction in RasE mice should give rise to eight genotypically different cell types with differential activation of Ras effector pathways (Fig. 2b).

For interpretation of cooperativities, stochastic activation of Ras mutant alleles would be a preferred situation in RasE mice to avoid under- or overrepresentation of certain cell types. In order to address the issue of a possible non-stochastic Cre/Lox-mediated bias in Ras effector activation, we generated transgenic embryonic stem cells with single integration of the RasE Multi-Hit BAC (ES^{RasE} cells). After transient transfection of a Cre expression plasmid, ES^{RasE} cells were subcloned and analysed for activation events. We observed subtle differences in allele activation but no major predominance of certain activation events suggesting stochastic activation of Ras mutant alleles (Suppl. Fig. 2).

The RasE Multi-Hit BAC was used for oocyte injection and F1 offsprings of RasE transgenic founders were analyzed for single copy integration (Suppl. Fig. 3a). The latter is important because presence of multiple copies would increase the background noise (i.e. activation events

that are not relevant for transformation) in tumors. RasE mice did not develop tumors within the time monitored (up to two years of age). We first crossed RasE mice with inducible Rosa26CreER^{T2} mice (RasE^{CreER})²¹ and demonstrated activation of M, R and P alleles after tamoxifen injection (Suppl. Fig. 3b). Consistently, Ras protein levels increased in certain tissues of RasE^{CreER} mice after tamoxifen treatment (Suppl. Fig. 3c).

Tumor spectrum in RasE^{CreER} mice after Cre-induction

Typical Ras-induced tumor types such as lung and pancreatic cancers were observed in 100% of RasE^{CreER} mice between 8 and 12 weeks after tamoxifen injection (Fig. 2c). Histopathologically, lung tumors appeared as adenocarcinomas whereas pancreatic tumors appeared as pancreatic intraepithelial neoplasias or pancreatic ductal adenocarcinomas (Fig. 2c). Moreover, tumors appeared in the skin of ~ 80% of mice that grew to a considerable size (Fig. 2c). IHC analysis suggested that they represent skin appendage tumors derived from sebaceous glands (Suppl. Fig. 4). No tumors were observed in age-matched RasE^{CreER} mice without tamoxifen injection (Fig. 2c).

We then investigated if tumor formation in RasE^{CreER} mice can be accelerated upon loss of a tumor suppressor protein such as PTEN. For that purpose, RasE^{CreER} mice were intercrossed with PTEN^{flox/flox} mice allowing random activation of Ras effector pathways and simultaneous loss of PTEN. Studies in tamoxifen-treated RasE^{CreER} PTEN^{flox/flox} mice showed a substantial cooperativity in tumorigenesis between activation of Ras effectors and loss of PTEN leading to a shortened lifespan of mice with PTEN deletion or PTEN haploinsufficiency (Figure 2d). Moreover, formation of lung and pancreatic tumors was substantially accelerated in RasE^{CreER} PTEN^{flox/flox} mice (Fig. 2e; data not shown). These data indicate cooperation between activation of Ras effector pathways and loss of PTEN in lung and pancreatic tumors.

Cooperation of Ras effector pathways in lung tumors

We focused on lung cancer for Ras effector pathway analysis because of the devastating prognosis of this malignant disease. To avoid interference by formation of other tumor types, we employed a lung-specific inhalation protocol using viral AdenoCre particles²². AdenoCre-treated RasE mice (RasE^{AdCre}) developed Pan-Cytokeratin-positive lung adenocarcinomas (Fig. 3a) but not pancreatic- or skin appendage tumors. Southern blot analysis of lung tissue shortly after AdenoCre treatment (6d) was not sensitive enough to detect activation of Ras mutant alleles (Fig.

3c) whereas PCR analysis was (data not shown). This suggests that only a small percentage of pulmonary epithelial cells are transiently infected with AdenoCre which is preferred to obtain focal tumors. In contrast, activation of Ras mutant alleles was readily detectable at a later stage (12we) when hyperplastic regions and tumors appeared (Fig. 3c). This suggests that positive selection resulted in enrichment of initiated and transformed cells that are most likely part of lung tumors. In order to address this issue, we have evaluated activation of Ras mutant alleles in lung tissue by in situ hybridization (ISH; Suppl. Fig. 5). ISH analysis confirmed activation of Ras mutant alleles in focal lung tumors (Fig. 3b). Determination of activation patterns in 190 lung tumors of 7 RasE^{AdCre} mice demonstrated that ~ 85% of tumors displayed simultaneous activation of M, R, and P (MRP tumors) whereas ~ 15% of lung tumors were derived from selected cells with a single or two activation events (non-MRP tumors; Fig. 3d). Among non-MRP tumors, P tumors were most frequently observed followed by MR and MP tumors. M and R tumors were rare and RP tumors were not present in RasE^{AdCre} mice (Fig. 3d).

We next addressed the question if the cooperative activation pattern of Ras effector pathways in lung cancer also appears in other tumor types and investigated pancreatic and skin appendage tumors. Tamoxifen-induced pancreatic tumors of RasE^{CreER} mice did not display a clear focal appearance but ISH analysis detected differential activation of Ras mutant alleles in several ductal structures of tumors suggesting a multifocal origin (data not shown). In contrast, skin appendage tumors grew as individual entities which facilitated determination of activation patterns. To avoid interference by formation of other tumor types, a skin-specific protocol using atopic application of 4-OH-tamoxifen onto the back skin²³ of RasE^{CreER} was applied. ISH analysis demonstrated that simultaneous activation of M, R and P was observed in 57 out of 58 skin appendage tumors (98,3%). Only a single tumor displayed activation of P only (Suppl. Fig. 6a). These data indicate that skin appendage tumors in RasE^{CreER} mice are strongly dependent on simultaneous activation M, R and P. Isolated skin appendage tumors were used for expression analysis of Ras mutant alleles using real-time PCR. These data confirmed activation of M, R and P and demonstrated that Ras mutant alleles are expressed at comparable levels in tumors (Suppl. Fig. 6b).

MAPK, RALGEF and PI3K Ras effector pathways cooperate in lung tumor invasiveness

Quantitation of tumor size in RasE^{AdCre} mice demonstrated that MRP lung tumors were slightly but insignificantly bigger than non-MRP lung tumors. Consistently, the number of mitotic figures

was moderately elevated in MRP lung tumors although Ki67-staining did not reveal major differences in proliferation between MRP and non-MRP tumors (data not shown). Given the minor importance of MRP activation for proliferation, we histopathologically characterized the impact of Ras effector pathways on tumor progression. All MRP and non-MRP lung tumors analyzed (~ 50) were negative for the Clara cell marker CC10 but positive for the type-II-pneumocyte marker SP-C and focally also SP-B (Fig. 4a; data not shown). Importantly, histopathological examination demonstrated that a substantial percentage of MRP tumors were invasive (Fig. 4b,d,e). Invasion occurred predominantly in the central part of MRP tumors. A characteristic desmoplastic stroma reaction²⁴ with newly formed blood vessels was observed and highlighted by Movat pentachrome-staining for matrix proteins and mesenchymal cells (Fig. 4d,e). In addition, MRP tumors showed either a solid or an acinar architecture (Fig. 4c). In contrast, non-MRP tumors were non-invasive (Fig. 4b,e) and showed a solid but no clear acinar architecture (Fig. 4c,e). Also mixed solid & acinar, solid & lepidic and lepidic tumors appeared. Further examination of non-MRP tumor subtypes P, MR and MP showed that the mixed solid & acinar architecture was only present in P tumors. These tumors grew into bronchi but did not induce desmoplastic stroma and blood vessel formation (data not shown).

Discussion

We have established a mouse model called Multi-Hit to identify gene cooperativities in cancer development. Using stochastic Cre-mediated activation and in vivo selection of specific genes of interest (GOIs), our model mimics evolution of cancers that have acquired synergistic mutations. Ideally, all cell types with alternative GOI combinations should be present at similar numbers after Cre activation to guarantee unbiased start conditions for tumor formation. Our experiments in ES^{RasE} cells suggested that there is no major Cre/LoxP-mediated bias that favours specific GOI combinations. Therefore, the Multi-Hit approach can be employed as a competitive in vivo test system for gene cooperativities in cancer formation that is based on positive and negative selection. The complexity of activation patterns can be substantially increased in double-transgenic Multi-Hit mice with two different Multi-Hit constructs (six different alleles give rise to 64 genotypically different cell types). We have tested the feasibility of such an approach and generated mice with the RasE Multi-Hit transgene and a second Multi-Hit construct harbouring three different constitutively active AKT mutants. Cre-mediated stochastic activation of the six alleles strongly accelerated formation and progression of various tumors when compared to single-transgenic RasE mice (data not shown).

Oncogenic Ras would be an ideal drug target but attempts to block Ras activity directly have proven disappointing²⁵. Given the limited druggability of Ras, surrounding drugs that inhibit crucial downstream signaling cascades of Ras might be more promising¹³. Constitutive active surrogate components such as MEK1^{Q56P} (for activation of MAPK), Rfl^{CAAX} (for activation of RALGEF) and PTEN shRNA (for activation of PI3K) have been used to dissect the requirement of individual Ras signaling pathways in tumorigenesis²⁶. More directly, H-ras mutant alleles V12S35, V12G37 and V12C40 have been developed that display selectivity for constitutive activation of MAPK, RALGEF or PI3K pathways, respectively^{12, 19, 20}. However, it should be considered that K-ras but not H-ras is the most frequently mutated Ras protein in human tumors² but no equivalent oncogenic K-ras alleles for selective activation of MAPK, RALGEF and PI3K effector pathways have been reported. Knock-in of H-ras into the endogenous K-ras locus rescued embryonic lethality of K-ras knockout mice indicating overlapping functions in development²⁷. We have identified typical K-ras-associated tumors in RasE^{CreER} mice such as lung and pancreatic cancers. Moreover, overlapping functions of H-ras and K-ras proteins have been described in fibroblast proliferation and immortalization although K-ras was quantitatively more efficient²⁶. These data suggest that the transforming potential of both Ras proteins is

mediated through the same downstream effector pathways and H-rasV12 mutant alleles can be (and have been) used as tools to study the requirement of Ras effectors in transformation²⁸⁻³¹.

Genetic data evaluating the importance of single Ras effector pathways during tumorigenesis in vivo are limited. The requirement for PI3K activation during initiation of lung tumor formation was demonstrated previously by genetic ablation of PI3K signaling in LSL K-ras^{G12D} mice^{32, 33}.

We observed cooperation potencies MAPK/RALGEF/PI3K > PI3K > MAPK/RALGEF > MAPK/PI3K > MAPK > RALGEF > RALGEF/PI3K in lung tumors of RasE^{AdCre} mice which underlines the requirement of PI3K activation. Interestingly, lung tumors with RP activation were not identified. The incompatibility between RALGEF and PI3K activation seems to depend on the status of MAPK activation which is supported by results in “Ras-less” cells. These cells lack H-ras and N-ras genes and contain floxed K-ras genes that have been conditionally deleted. Coexpression of Rfl^{CAAX} (for activation of RALGEF) and PTEN shRNA (for activation of PI3K) failed to induce colony formation in Ras-less cells whereas coexpression of Rfl^{CAAX}, PTEN shRNA and MEK1^{Q56P} (for additional activation of MAPK) potently induced colony formation²⁶. Precursor cells with activation of all three Ras effectors were most potently selected in RasE^{AdCre} and gave rise to invasive MRP lung adenocarcinomas. In contrast, non-MRP tumors did not display an invasive histopathology. Among Ras effector pathways, mainly Ras-mediated activation of ERK but also PI3K and RALGEF have been considered to promote invasiveness of tumor cells^{34, 35}. In our experimental setup, activation of all three Ras effector alleles was required for invasiveness of RasE^{AdCre} lung tumors.

In summary, we have established a Multi-Hit mouse model for investigation of genetic interactions in cancer formation and used Ras signaling in lung tumors as a paradigm. The juxtaposed presence of different tumors in individual lungs allowed a side by side correlation between the induced genetic status (Cre-mediated activation events) and important tumor parameters such as proliferation and invasiveness. The possibility to generate double-transgenic mice harbouring two different Multi-Hit transgenes might also facilitate development of complex mouse models (e.g. for tumor metastasis). Future experiments in RasE mice will show if pathway interactions are altered by tumor suppressor functions frequently lost during tumor progression and if these findings can be extrapolated for prediction of drug treatment efficacies.

Methods

Generation of RasE Multi-Hit mice

The RasE Multi-Hit transgene consisted of three independent expression modules, each containing the CAGGS promoter, the gene of interest (H-rasV12 effector mutants S35, G37, and C40)^{19, 20}, an IRES (5xGtx)³⁶, a reporter gene (EYFP, dsRed, hCD2t) and a SV40 polyadenylation signal. All modules are flanked by chicken 2xHS4 insulator sequences³⁷. A BAC recombineering strategy that is described in detail in Figure 1 was used for assembly of Multi-Hit constructs. The genes of interest are cloned using unique restriction enzymes (8-cutters) thereby allowing easy exchange for other genes of interest. The RasE Multi-Hit transgene was recombined into the PstI restriction site of the murine Collagen1a1 BAC used previously for integration of transgenes because of its open chromatin structure³⁸. RasE mice were generated by pronuclear injection of oocytes and 5 founders [B6;D2-Tg(RasE)289-293Biat] were identified by Southern blot and PCR. F1 offsprings of founder Tg290 were analyzed by Southern blot demonstrating single copy integration of the RasE BAC. RasE mice were bred with Rosa26CreER^{T2} and PTEN^{flox/flox} mice^{21, 39} to generate compound mouse models that were kept on a mixed background (C57BL/6x129). Only littermates were used for experiments. For all animal studies were performed in accordance with Austrian and European laws and with the general regulations specified by the Good Scientific Practices guidelines of the Medical University of Vienna.

Tamoxifen and AdenoCre administration

Mice were injected intraperitoneally on 1 to 5 consecutive days with 1mg of the Tamoxifen free base (T5648, Sigma) dissolved in sun flower seed oil (Fluka). For atopic application, 1mg of 4OH-Tamoxifen (Sigma), dissolved in 100% ethanol was applied on the shaved back-skin of mice²³. Lung application of AdenoCre was performed through intranasal instillation using an AdenoCre-CaCl₂ precipitate²². For AdenoCre-CaCl₂ precipitation, 60µl MEM, 2.5 µl AdenoCre solution (10¹⁰ pfu/ml; University of Iowa, gene Transfer Vector Core) and 0.6 µl CaCl₂ were mixed for each mouse and incubated 20 min at room temperature.

Histology, immunohistochemistry (IHC) and *in situ* hybridisation

Tissues were fixed in 4% buffered formaldehyde. 2 µm thick paraffin sections were used for H&E staining, Movat pentachrome-staining and IHC using standard procedures. Immunohistochemistry was performed using antibodies against CK7 (ab90221, Abcam), Pan CK (MS-343-P0, Thermo Fisher Scientific), HMWCK (MO630, Dako Cytomation), N-Cam (NCL-CD56-1B6, Novocastra), CC10 (25555, Santa Cruz), SP-C (13979, Santa Cruz). *In situ* hybridisation was performed by incubating 2 µm paraffin sections with *in vitro* transcribed sense and antisense digoxigenin (DIG -11-UTP) (11209256910, Roche) labelled RNA probes against the EYFP, dsRed and hCD2t in hybridisation solution (10mM Tris (pH 7.5), 600mM NaCl, 1mM EDTA, 0.25% SDS, 10% Dextran Sulfate, 1x Denhardt's buffer, 200µg/µL yeast tRNA, 50% Formamide) for 36 hours at 65°C. Anti-Digoxigenin-AP, Fab fragments (11093274910, Roche) were used to detect the digoxigenin labelled RNA probes. Colour development was carried out using BM purple substrate (11442074001, Roche), followed by nuclear counterstaining with 0.05% nuclear fast red (N069.1, Carl Roth GmbH, Germany). H&E-stained and *in situ* hybridised slides were scanned using TissueFaxs™ software (TissueGnostics GmbH, www.tissuegnostics.com). Tumor grading was performed by a board certified pathologist (HP).

PCR analysis

PCR analysis for activation of expression modules was performed with a primer in the CAGGS promoter and a primer located in the individual signature sequence following the genes of interest. This strategy detected only activated expression modules. For realtime PCR, an Eppendorf light cycler was used and amplicons were detected with SYBR Green (Roche Diagnostics). The expression levels of transcripts were calculated with the comparative CT (threshold concentration) method. The individual RNA levels were normalized for gapdh and are depicted as relative expression values.

Southern Blot and Western Blot

For Southern blot analysis, tail DNA of F1 offsprings of Tg(RasE)290BIAT was digested with EcoRI and probed with a fragment matching the Collagen1a1 locus. Genomic DNA from organs treated with Tamoxifen and AdenoCre was digested with XcmI for detection of modules 1 and 2 and HindIII for detection of module 3. DNA fragments for EYFP, dsRed and hCD2t were used as probe. Western Blot analysis was performed with whole cell protein extracts from organs using

standard protocols. Membranes were incubated with antibodies against Pan-Ras (OP40, Calbiochem) and HSC70 (Santa Cruz, 7298).

Statistics

All values are represented as means \pm s.e.m.. Statistical analysis was performed using the student's t test and a P value below 0.05 was considered significant.

Figure legends

Figure 1: Principle of the Multi-Hit tumor mouse. (a) Scheme of a transgenic Multi-Hit construct for three hits (upper drawing). The hits represent expression modules for oncogenes (or expression modules for knock-down of tumor suppressor genes). The expression modules (Hit 1,2,3) are cloned in inverted (off) orientations behind a promoter (arrow). Each expression module is flanked by loxP sites (triangles) that allow Cre-mediated activation (flipping). Incompatible, heterotypic loxP sites (black = canonical loxP; blue = lox5171; red = lox2272) are used to avoid deletions. Upon transient induction of Cre, expression modules flip until Cre activity ceases. Then, they remain either in on- or in off-orientations. Therefore, Cre induction in a Multi-Hit mouse results in stochastic activation of expression modules creating 8 genotypically different cell types (lower drawing). Combinations of synergistic hits are positively selected and should result in tumors. (b) Recombineering strategy for Multi-Hit BAC constructs. 1) Vector 1 containing expression module 1 (Hit 1) is integrated via ET recombination into the BAC. Module 1 is flanked by FRT recombination sites and chicken 2xHS4 insulator sequences that avoid promoter interference and promoter suppression. Together with the module 1, an ampicillin resistance gene (Amp) flanked by Φ C31 attB recombination sites is integrated and recombinants are selected for ampicillin resistance. 2) Vector 2 containing expression modules 2, 3 (Hit 2,3) and a kanamycin resistance gene (Neo) is integrated into the BAC via Φ C31 attP recombination. Recombinants are screened for loss of ampicillin and gain of kanamycin resistance. The resulting construct contains all expression modules (not shown in detail) flanked by chicken 2xHS4 insulators. The whole locus is flanked by FRT recombination sites that allows FLP-mediated deletion to address oncogene addiction.

Figure 2: The RasE (Ras effector) Multi-Hit mouse model. (a) Schemes of the RasE Multi-Hit BAC (upper drawing) and individual expression modules (lower drawings). Cre-mediated inversion can be followed by PCR using a primer in the promoter (black arrow) and individual primers binding to unique sequences (blue, green and red arrows). FRT: FRT recombination site; 2xHS4: chicken 2xHS4 insulator; attL, attR: sequences generated during assembly of the BAC by Φ C31 recombination; P: CAGGS promoter; S35, G37, C40: pathway-specific H-rasV12 mutants; Gtx: IRES; EYFP, dsRed, hCD2t: reporter genes; pA: SV40 polyadenylation signal; triangles: heterotypic loxP sites. (b) Possible activation events in cells of RasE Cre double-transgenic mice.

(c) Tumor formation in $RasE^{CreER}$ mice 12 weeks after tamoxifen treatment (tam). Lung tumors were visible as focal lesions (arrows in upper middle image; bar = 1mm; upper right image represents higher magnification of a tumor; bar = 0.1mm). Pancreatic tumors (lower middle image; bar = 1mm) stained positive for Cytokeratin 7 (red; right inset; left inset represents a non-tumorigenic pancreatic region). Skin appendage tumors (lower right image; bar = 0.1mm; inset indicates normal skin) grew to a considerable size (macroscopic view). No tumor formation was observed in lungs (upper left image; bar = 1mm) and pancreas (lower left image; bar = 1mm) of untreated age-matched $RasE^{CreER}$ mice (no tam). T: tumor; S: tumor stroma. (d) Kaplan Meier plot of $RasE^{CreER}$, $RasE^{CreER} PTEN^{flox/+}$ and $RasE^{CreER} PTEN^{flox/flox}$ mice after tamoxifen treatment. (e) Lung tumors (arrowheads) in $RasE^{CreER}$, $RasE^{CreER} PTEN^{flox/+}$ and $RasE^{CreER} PTEN^{flox/flox}$ mice 8 weeks after tamoxifen treatment. Upper and lower left images represent macroscopic views. Lower right image represents higher magnification of a tumor (rectangle in lower left image) in $RasE^{CreER} PTEN^{flox/flox}$ mice.

Figure 3: Lung adenocarcinomas in $RasE^{AdCre}$ mice. (a) Tumors (arrowheads) on a lung 18 weeks after AdenoCre administration (left image) grew as as focal lesions (middle image) and stained positive for Pan-Cytokeratin (right image; inset represents a tumor to normal tissue boundary at higher magnification). (b) ISH analysis of lung tumors with probes specific for activated M, R and P (activation in blue). MR tumors (M and R activation) and P tumors (activation of P only) are indicated by black and red circles, respectively. The insets show a higher magnification of a MR and P tumor. (c) Southern blot performed with lung tissue after short-term AdenoCre treatment (6 days) and after tumors have developed (12 weeks). (d) Activation patterns of M, R and P in lung tumors of $RasE^{AdCre}$ mice (7 mice; 190 tumors).

Figure 4 : Histopathological evaluation of lung tumors. (a) IHC-staining of $RasE^{AdCre}$ lung tumors for the clara cell marker CC10 and the type-II-pneumocyte marker SP-C. T: tumor. (b,c) 29 MRP tumors and 29 non-MRP tumors were histopathologically analysed for invasiveness (B) and tumor architecture (c). (d) Invasive acinar MRP carcinoma (T1095) with desmoplastic stroma (S) in the center (left image and third image from the left). Presence of newly formed tumor stroma was confirmed by Movat pentachrome-staining (right image). Higher magnification demonstrated growth into bronchi (arrowheads) and establishment of tumor blood vessels (second image from the left). (e) Examples of non-MRP tumors. Non-invasive P tumors (T1183

and T71) growing into bronchi (upper left and upper right images) but respecting the blood boundary (arrowheads in upper middle image). Mixed solid&acinar tumor architecture of a P tumor (T1102; lower left and middle images). High grade MP tumor (T1026) with high nuclear/cytoplasmic ratio. Low and high-grade in-situ carcinomas were discerned based on nuclear/cytoplasmic ratios and the presence or absence of large granules within the cytoplasm (lamellar bodies). (f) Summary of Ras effector pathway cooperations in lung tumorigenesis.

Acknowledgements

We thank Julian Downward for Ras effector mutants, Anton Berns for Rosa26CreER^{T2} mice and Gary Felsenfeld for chicken 2xHS4 insulator sequences. We thank Maria Sibilina and Erwin F. Wagner for critical reading of the manuscript and Markus Mair and Deeba Khan for technical assistance. This work was supported by the Ludwig Boltzmann Gesellschaft LBG, the Austrian Science Fund FWF grant SFB F28 to MM, RM and RE, the FWF DK-plus grant IAI to MM and RE, the CCC Research Grant to EC and RE and the Austrian Federal Ministry of Science and Research GENAU grant “Austromouse” to MM, TR, JP, EC and RE.

References

1. Diaz-Flores, E. & Shannon, K. Targeting oncogenic Ras. *Genes & development* **21**, 1989-1992 (2007).
2. Downward, J. Targeting RAS signalling pathways in cancer therapy. *Nature reviews* **3**, 11-22 (2003).
3. Giehl, K. Oncogenic Ras in tumour progression and metastasis. *Biological chemistry* **386**, 193-205 (2005).
4. Karnoub, A.E. & Weinberg, R.A. Ras oncogenes: split personalities. *Nat Rev Mol Cell Biol* **9**, 517-531 (2008).
5. Malumbres, M. & Barbacid, M. RAS oncogenes: the first 30 years. *Nature reviews* **3**, 459-465 (2003).
6. Repasky, G.A., Chenette, E.J. & Der, C.J. Renewing the conspiracy theory debate: does Raf function alone to mediate Ras oncogenesis? *Trends in cell biology* **14**, 639-647 (2004).
7. Moodie, S.A., Willumsen, B.M., Weber, M.J. & Wolfman, A. Complexes of Ras.GTP with Raf-1 and mitogen-activated protein kinase kinase. *Science (New York, N.Y)* **260**, 1658-1661 (1993).
8. Vojtek, A.B., Hollenberg, S.M. & Cooper, J.A. Mammalian Ras interacts directly with the serine/threonine kinase Raf. *Cell* **74**, 205-214 (1993).
9. Warne, P.H., Viciano, P.R. & Downward, J. Direct interaction of Ras and the amino-terminal region of Raf-1 in vitro. *Nature* **364**, 352-355 (1993).
10. Zhang, X.F. et al. Normal and oncogenic p21ras proteins bind to the amino-terminal regulatory domain of c-Raf-1. *Nature* **364**, 308-313 (1993).
11. Khosravi-Far, R. et al. Oncogenic Ras activation of Raf/mitogen-activated protein kinase-independent pathways is sufficient to cause tumorigenic transformation. *Molecular and cellular biology* **16**, 3923-3933 (1996).
12. Rangarajan, A., Hong, S.J., Gifford, A. & Weinberg, R.A. Species- and cell type-specific requirements for cellular transformation. *Cancer cell* **6**, 171-183 (2004).
13. McCormick, F. Cancer therapy based on oncogene addiction. *Journal of surgical oncology* **103**, 464-467.
14. Hanahan, D. & Weinberg, R.A. Hallmarks of cancer: the next generation. *Cell* **144**, 646-674.
15. Hanahan, D. & Weinberg, R.A. The hallmarks of cancer. *Cell* **100**, 57-70 (2000).
16. Mantovani, A. Cancer: Inflaming metastasis. *Nature* **457**, 36-37 (2009).
17. Blaas, L., Musteanu, M., Zenz, R., Eferl, R. & Casanova, E. PhiC31-mediated cassette exchange into a bacterial artificial chromosome. *BioTechniques* **43**, 659-660, 662, 664 (2007).
18. Zhang, Y., Buchholz, F., Muyrers, J.P. & Stewart, A.F. A new logic for DNA engineering using recombination in Escherichia coli. *Nature genetics* **20**, 123-128 (1998).
19. Joneson, T., White, M.A., Wigler, M.H. & Bar-Sagi, D. Stimulation of membrane ruffling and MAP kinase activation by distinct effectors of RAS. *Science (New York, N.Y)* **271**, 810-812 (1996).
20. White, M.A. et al. Multiple Ras functions can contribute to mammalian cell transformation. *Cell* **80**, 533-541 (1995).
21. Hameyer, D. et al. Toxicity of ligand-dependent Cre recombinases and generation of a conditional Cre deleter mouse allowing mosaic recombination in peripheral tissues. *Physiological genomics* **31**, 32-41 (2007).

22. DuPage, M., Dooley, A.L. & Jacks, T. Conditional mouse lung cancer models using adenoviral or lentiviral delivery of Cre recombinase. *Nature protocols* **4**, 1064-1072 (2009).
23. Vasioukhin, V., Degenstein, L., Wise, B. & Fuchs, E. The magical touch: genome targeting in epidermal stem cells induced by tamoxifen application to mouse skin. *Proceedings of the National Academy of Sciences of the United States of America* **96**, 8551-8556 (1999).
24. Dingemans, K.P. & Mooi, W.J. Ultrastructure of tumour invasion and desmoplastic response of bronchogenic squamous cell carcinoma. *Virchows Archiv* **411**, 283-291 (1987).
25. Downward, J. Signal transduction. Prelude to an anniversary for the RAS oncogene. *Science (New York, N.Y)* **314**, 433-434 (2006).
26. Drosten, M. et al. Genetic analysis of Ras signalling pathways in cell proliferation, migration and survival. *The EMBO journal* **29**, 1091-1104.
27. Potenza, N. et al. Replacement of K-Ras with H-Ras supports normal embryonic development despite inducing cardiovascular pathology in adult mice. *EMBO reports* **6**, 432-437 (2005).
28. Campbell, P.M. & Der, C.J. Oncogenic Ras and its role in tumor cell invasion and metastasis. *Seminars in cancer biology* **14**, 105-114 (2004).
29. Janda, E., Litos, G., Grunert, S., Downward, J. & Beug, H. Oncogenic Ras/Her-2 mediate hyperproliferation of polarized epithelial cells in 3D cultures and rapid tumor growth via the PI3K pathway. *Oncogene* **21**, 5148-5159 (2002).
30. Janda, E. et al. Raf plus TGFbeta-dependent EMT is initiated by endocytosis and lysosomal degradation of E-cadherin. *Oncogene* **25**, 7117-7130 (2006).
31. Webb, C.P., Van Aelst, L., Wigler, M.H. & Woude, G.F. Signaling pathways in Ras-mediated tumorigenicity and metastasis. *Proceedings of the National Academy of Sciences of the United States of America* **95**, 8773-8778 (1998).
32. Engelman, J.A. et al. Effective use of PI3K and MEK inhibitors to treat mutant Kras G12D and PIK3CA H1047R murine lung cancers. *Nature medicine* **14**, 1351-1356 (2008).
33. Gupta, S. et al. Binding of ras to phosphoinositide 3-kinase p110alpha is required for ras-driven tumorigenesis in mice. *Cell* **129**, 957-968 (2007).
34. Doehn, U. et al. RSK is a principal effector of the RAS-ERK pathway for eliciting a coordinate promotile/invasive gene program and phenotype in epithelial cells. *Molecular cell* **35**, 511-522 (2009).
35. Mishra, P.J. et al. Dissection of RAS downstream pathways in melanomagenesis: a role for Ral in transformation. *Oncogene* **29**, 2449-2456.
36. Chappell, S.A., Edelman, G.M. & Mauro, V.P. Biochemical and functional analysis of a 9-nt RNA sequence that affects translation efficiency in eukaryotic cells. *Proceedings of the National Academy of Sciences of the United States of America* **101**, 9590-9594 (2004).
37. Yusufzai, T.M. & Felsenfeld, G. The 5'-HS4 chicken beta-globin insulator is a CTCF-dependent nuclear matrix-associated element. *Proceedings of the National Academy of Sciences of the United States of America* **101**, 8620-8624 (2004).
38. Hochedlinger, K., Yamada, Y., Beard, C. & Jaenisch, R. Ectopic expression of Oct-4 blocks progenitor-cell differentiation and causes dysplasia in epithelial tissues. *Cell* **121**, 465-477 (2005).
39. Suzuki, A. et al. T cell-specific loss of Pten leads to defects in central and peripheral tolerance. *Immunity* **14**, 523-534 (2001).

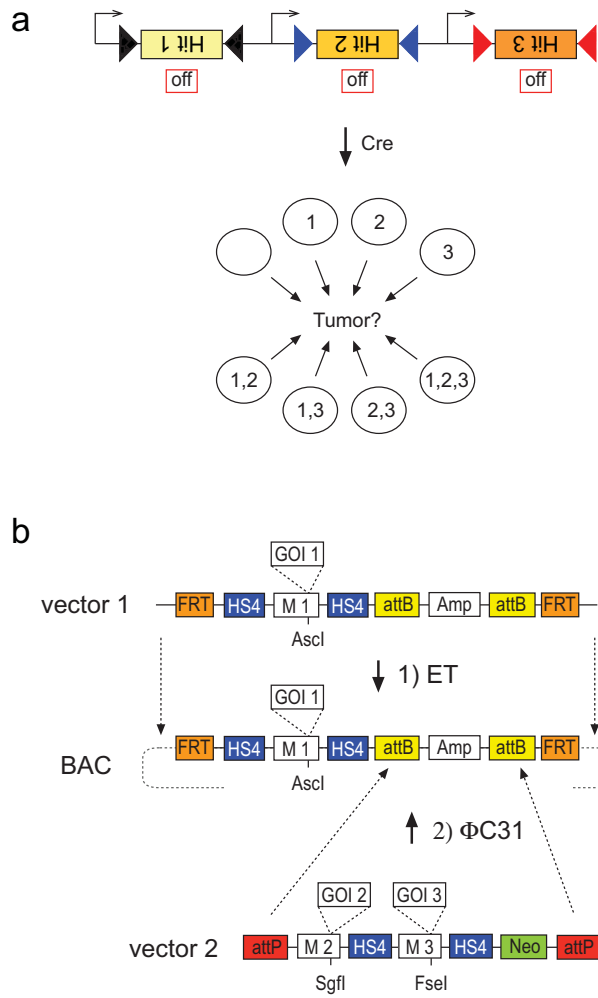


Figure 1

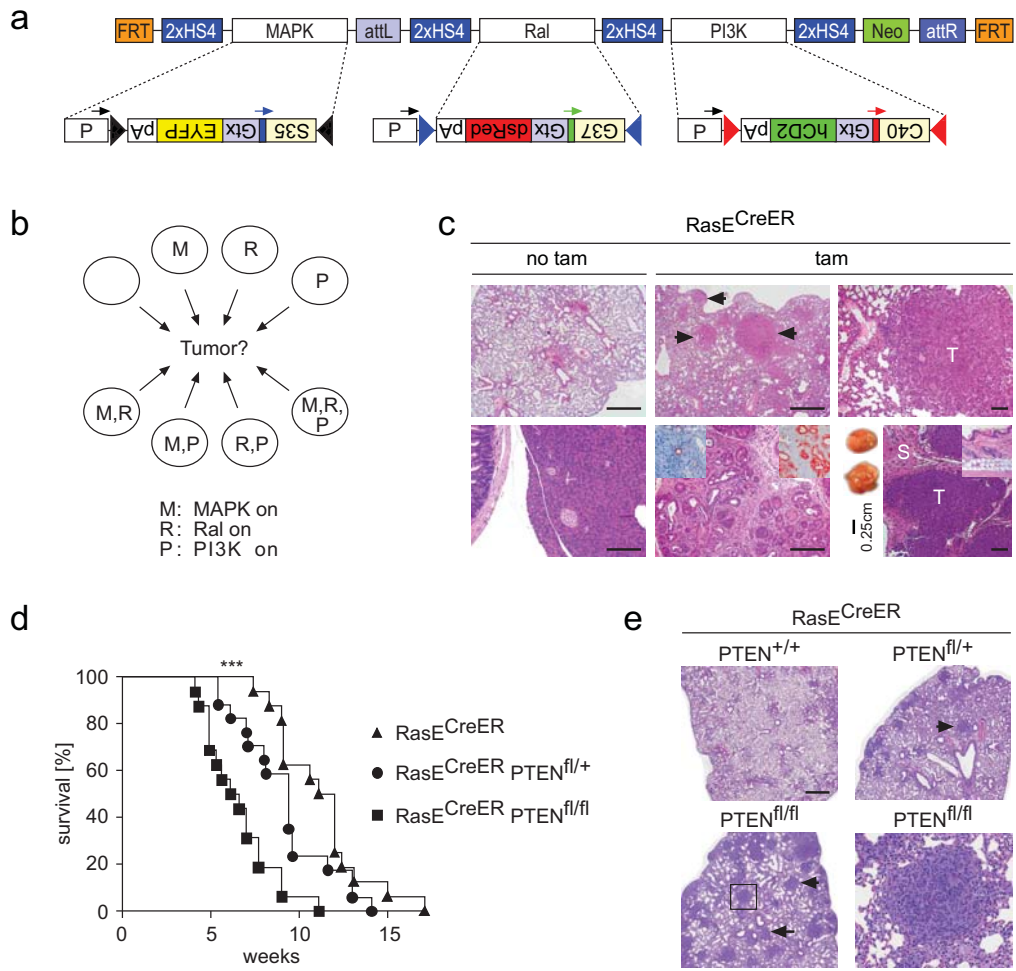


Figure 2

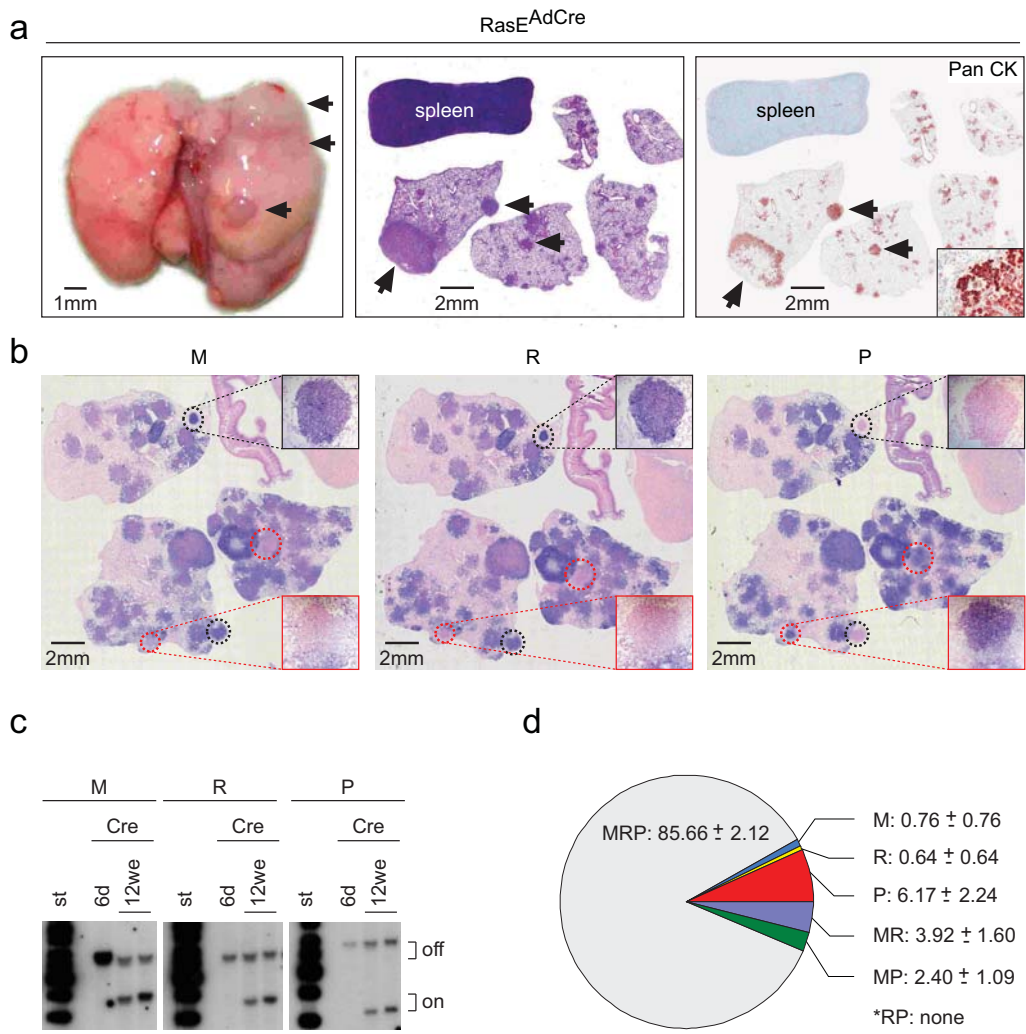


Figure 3

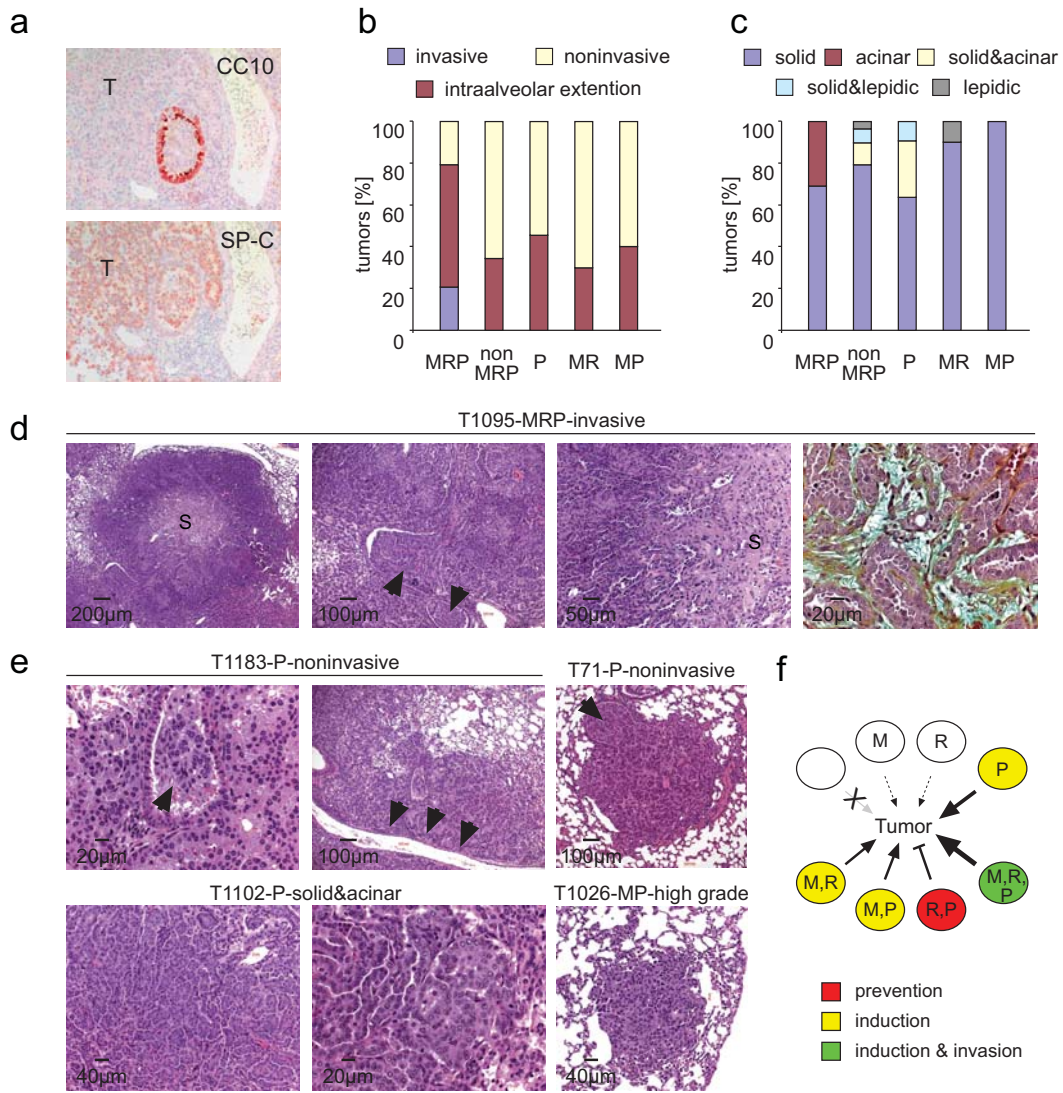


Figure 4